



Stepwise synthesis and properties of a 9,10-dihydro-9,10-diboraanthracene

Tomohiro Agou^{a,b}, Masaki Sekine^c, Takayuki Kawashima^{c,*}

^a Kyoto University Pioneering Research Unit for Next Generation, Kyoto University, Gokasho, Uji 611-0011, Japan

^b Institute for Chemical Research, Kyoto University, Gokasho, Uji 611-0011, Japan

^c Department of Chemistry, Graduate School of Science, The University of Tokyo, 7-3-1 Hongo, Bunkyo-ku, Tokyo 113-0033, Japan

ARTICLE INFO

Article history:

Received 27 April 2010

Revised 9 July 2010

Accepted 14 July 2010

Available online 16 July 2010

ABSTRACT

A stepwise synthetic method for a 9,10-dihydro-9,10-diboraanthracene was developed, and the optical and electrochemical properties as well as the molecular structure of the 9,10-dihydro-9,10-diboraanthracene were elucidated. The 9,10-dihydro-9,10-diboraanthracene exhibited high complexation ability against fluoride ion, and the complexation was accompanied by the enhancement of photoluminescence emission, probably due to intramolecular charge transfer between the two boron atoms.

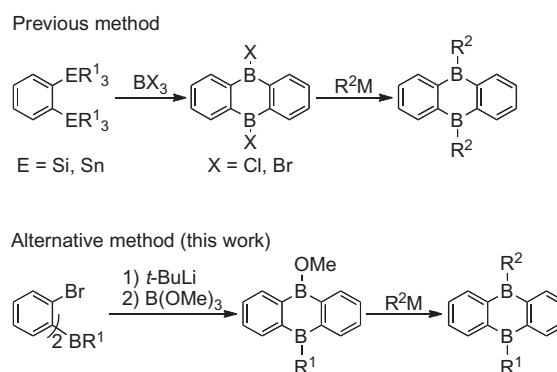
© 2010 Elsevier Ltd. All rights reserved.

π -Conjugated molecules bearing boron atoms as electron- or Lewis base acceptors have been investigated extensively as multi-functional organic materials for organic semi-conductors, photonics, and chemosensors,¹ and the accumulation of boron atoms in conjugated systems is expected to improve these characteristics effectively.² A 1,4-diborin has two boron atoms in a cyclohexadiene ring, and thus the strong electronic interaction between the boron atoms through the π -orbitals is anticipated. Several dibenzo-fused 1,4-diborin derivatives, 9,10-dihydro-9,10-diboraanthracenes were synthesized, and their properties were investigated including electron acceptability,³ charge transfer complex formation with electron donors (e.g., TTF),^{3b,c} activation of olefin polymerization catalyst,⁴ photo-luminescence,⁵ and complexation behavior to Lewis bases⁶ or transition metals.⁷ Owing to these attractive features, 9,10-dihydro-9,10-diboraanthracenes will be applied to molecular devices by the incorporation of proper functional groups, like electron-donating substituents.

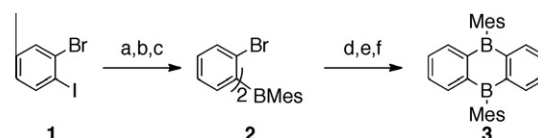
One drawback in the development of functionalized 9,10-dihydro-9,10-diboraanthracenes is the lack of a general synthetic method. As shown in Scheme 1, previous synthetic methods employed transmetallation of silicon or tin atoms to boron atoms using BX_3 , quite a strong Lewis acid.⁸ Acid-sensitive functional groups can not be tolerated under such harsh conditions.

In this Letter, we describe a new and simple synthetic methodology for a 9,10-dihydro-9,10-diboraanthracene framework under ambient conditions where various functional groups can resist (Scheme 1, bottom). In addition, the molecular structure, optical properties, electrochemical properties, and complexation abilities of a 9,10-dihydro-9,10-diboraanthracene are also reported.

Synthesis of 9,10-dihydro-9,10-diboraanthracene **3** is shown in Scheme 2.⁹ 1-Bromo-2-iodobenzene (**1**) was converted to the corresponding Grignard reagent using *i*-PrMgCl and treated with $B(OMe)_3$ to give an intermediate borinic ester. This borinic ester was reacted with MesMgBr to afford triarylborane **2** in a moderate yield. In the second step, **2** was treated with *t*-BuLi, $B(OMe)_3$ and MesMgBr successively to give 9,10-dihydro-9,10-diboraanthracene



Scheme 1. Comparison of two synthetic methods of 9,10-dihydro-9,10-diboraanthracenes.



Scheme 2. Synthesis of 9,10-dihydro-9,10-diboraanthracene **3**. Reagents and conditions: (a) *i*-PrMgCl, THF, $-78\text{ }^\circ\text{C}$; (b) $B(OMe)_3$, $-78\text{ }^\circ\text{C}$ to rt; (c) MesMgBr, reflux, 55% over three steps; (d) *t*-BuLi, $-78\text{ }^\circ\text{C}$, Et_2O ; (e) $B(OMe)_3$, $-78\text{ }^\circ\text{C}$ to rt; (f) MesMgBr, THF, reflux; 47% over three steps.

* Corresponding author at Present address: Faculty of Science, Gakushuin University, 1-5-1 Mejiro, Toshima-ku, Tokyo 171-8588, Japan. Tel.: +81 3 3986 0221.

E-mail address: Takayuki.Kawashima@gakushuin.ac.jp (T. Kawashima).

3. Compounds **2** and **3** were obtained as colorless and pale yellow solids, respectively, and both boranes can be handled and stored under air.

Single crystals of **3** were obtained by slow evaporation of a saturated Et₂O solution, and its molecular structure was elucidated by X-ray crystallographic analysis (Fig. 1).¹⁰ The fused benzene rings did not show large bond alternation (1.39–1.43 Å), and the B–C bond lengths are in the range of typical B(sp²)-C(aryl) bond lengths (cf. 1.57–1.59 Å in BPh₃).¹¹ These structure parameters are comparable to those of a 9,10-dihydro-9,10-diboraanthracene bearing methyl groups on the boron atoms^{3c,7b} and indicate that the contribution of cyclic π -electron delocalization over the central diborin ring is marginal, and thus the electronic structure of the diborin ring of **3** can be classified as a non-aromatic rather than a 4 π anti-aromatic. A NICS(1) value calculated on model compound **3'** (+3.5) also indicated that the diborin ring of **3** has only weak anti-aromaticity.¹² In contrast, 1,2-diborins were reported to have substantial anti-aromatic character, and thus the position of the boron atoms in the six-membered ring systems should affect the electronic structure substantially.¹³

UV-vis and fluorescence spectra of **3** were recorded in cyclohexane and THF (Fig. 2). Compound **3** showed a strong absorption band at 349 nm bearing a small shoulder in both the solvents.¹⁴ This strong absorption was attributed to the π - π^* excitations of the 9,10-dihydro-9,10-diboraanthracene, on the basis of TD-DFT calculations (λ_{calcd} 339 nm, f 0.1253).¹⁵ The calculations also indicated that **3** has several forbidden excitations at lower energy levels (λ_{calcd} 442, 422, 409, 408, 377 nm), which can be described as an intramolecular charge transfer from the electron-rich mesityl groups to the electron-accepting 9,10-dihydro-9,10-diboraanthracene ring. The observed shoulder-like absorption around 400 nm is thought to correspond to these forbidden transitions. Small

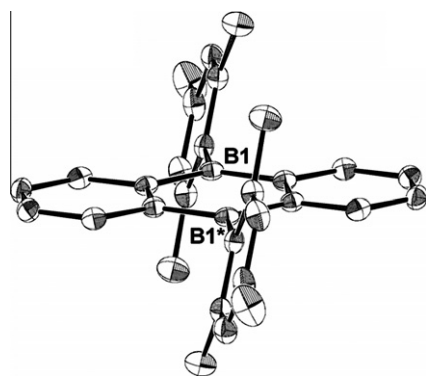


Figure 1. Thermal ellipsoid plot of **3** (50% probability level). Hydrogen atoms are omitted. Selected bond lengths (Å) and angles (°): B–C(Ar), 1.560(2), 1.571(2); B–C(Mes), 1.589(2); C(Ar)–B–C(Ar), 118.33(12); C(Ar)–B–C(Mes), 120.08(12), 121.59(13).

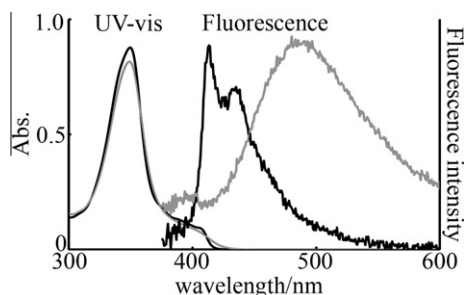


Figure 2. UV-vis and fluorescence spectra of **3**. Black line: in cyclohexane. Gray line: in THF.

red-shift of the absorption tail in THF may reflect the nature of the intramolecular charge transfer absorption.

In cyclohexane, **3** exhibited a fluorescence emission centered at 413 nm (Φ 0.02). Small Stokes shift (<10 nm) indicates the molecular rigidity of the optically excited **3**. Changing the solvent from cyclohexane to THF resulted in a red shift of the emission maximum by 70 nm and a broadening of the band shape (λ_{em} 483 nm, Φ 0.05). These results suggest that the emissive state of **3** is highly polarized. As described above, the lowest excited state of **3** is an intramolecular charge transfer state, which is effectively stabilized in more polar THF, resulting in the observed solvatochromic shift. Because the radiative de-activation from this state is symmetrically forbidden ($f = 0$), the fluorescence quantum yields were small.

The electron acceptability of **3** was investigated by using cyclic voltammetry. The measurements were performed in THF containing (*n*-Bu)₄N ClO₄ (0.1 M) as a supporting electrolyte at 298 K with a scan rate of 0.1 V s⁻¹ (Fig. 3). Compound **3** exhibited two reversible one-electron reduction waves at $E_{1/2} = -1.82$ and -2.78 V (vs Cp₂Fe/Cp₂Fe⁺), indicating the generation of radical anion and dianion, respectively. The shape of the voltammogram did not change after five cycles, suggesting the durability of the anionic species. Because the first reduction occurred at a much lower potential compared with that of Mes₃B ($E_{1/2} = -2.79$ V), **3** should work as a good electron acceptor. Meanwhile, the enhanced electron acceptability of **3** suggested its high Lewis acidity, and thus we next investigated the complexation ability of **3** against fluoride ion, a typical Lewis base against boron Lewis acids.

In THF, **3** (5.2×10^{-5} M) was mixed with a THF solution of (*n*-Bu)₄NF, and the reaction was monitored with UV-vis and fluorescence spectroscopy (Fig. 4a). The addition of fluoride ion (up to 1 equiv vs **3**) resulted in the decay of the absorption band around 349 nm and in the development of a new band centered at 280 nm with a set of isosbestic points. The new band was assigned to an intramolecular charge transfer absorption between the fluoroborate moiety and the trivalent boron atom in [3-F]⁻, judging from TD to DFT calculation on model compound [3'-F]⁻ (λ_{calcd} 378 nm). The increase in the absorption ceased, when just 1 equiv of fluoride ion was added, revealing that the formation of [3-F]⁻ was quantitative in this condition which was also shown by the large complexation constant ($K = 2(1) \times 10^8$ M⁻¹).¹⁶ Further addition of fluoride ion resulted in the decrease in the absorption of [3-F]⁻, but this change did not finish even after the addition of 3 equiv of fluoride ion. Another isosbestic point was observed at 246 nm, suggesting that this spectral change is corresponding to the conversion of [3-F]⁻ to another species rather than the decomposition of [3-F]⁻.¹⁷

The complexation could also be monitored with fluorescence spectroscopy (Fig. 4b). Corresponding to the blue shift of the UV-vis absorption, the emission maximum also showed hypsochromic shift from 483 to 400 nm. Although the absorbance at the excitation light (λ_{ex} 348 nm) decreased steeply (Fig. 4a), apparent fluo-

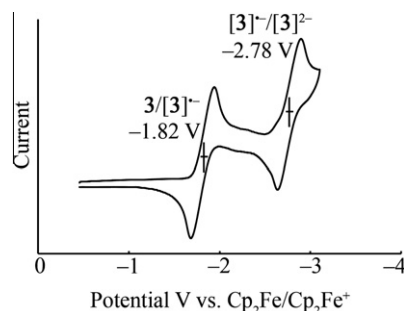


Figure 3. Cyclic voltammogram of **3**.

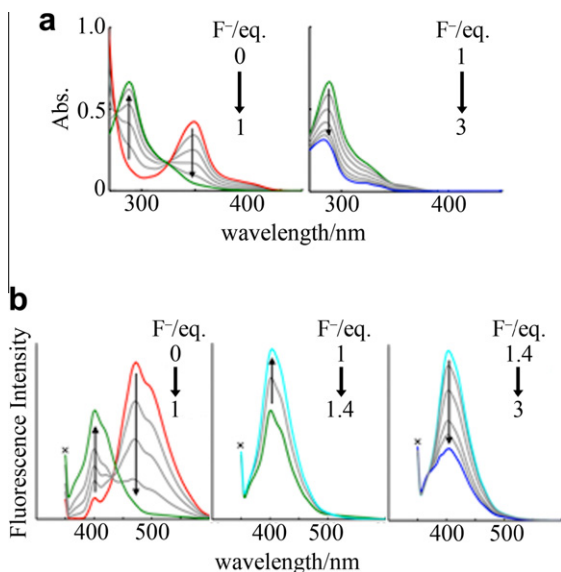


Figure 4. UV-vis and fluorescence spectral change of **3** ($[3] = 5.2 \times 10^{-5} \text{ M}$) upon addition of $(n\text{-Bu})_4\text{NF}$ in THF at 298 K. (a) UV-vis spectra. (b) Fluorescence spectra. The X marks indicate scattered excitation light (348 nm).

rescence intensity did not change very much. Therefore, the fluorescence quantum yield itself should improve by the formation of $[3\text{-F}]^-$. In fact, the quantum yield was estimated to be 0.15, when 1 equiv of fluoride ion was added.¹⁸ Interestingly, addition of excess fluoride ion enhanced the emission intensity (Fig. 4b, middle), and the fluorescence quantum yield reached 0.24 or 0.37 upon addition of 1.4 equiv or 2.0 equiv of fluoride ion, respectively. Because the formation of $[3\text{-F}]^-$ was completed by addition of 1 equiv of fluoride ion, the emission enhancement should not originate from the progress of the formation of $[3\text{-F}]^-$. The origin of this strange behavior is still unclear.

In conclusion, the stepwise synthetic route to the 9,10-dihydro-9,10-diboraanthracene was developed. This method can be utilized for the synthesis of 9,10-dihydro-9,10-diboraanthracene derivatives bearing acid-sensitive functional groups. The 9,10-dihydro-9,10-diboraanthracene has a planar structure, and the central diboron ring is classified as a non-aromatic system on the basis of crystallographic analysis and GIAO calculations. UV-vis and fluorescence spectroscopy as well as theoretical calculations revealed that unique photo-physical characteristics of the 9,10-dihydro-9,10-diboraanthracene, and electrochemical measurement showed the enhanced electron-accepting property of this compound. The 9,10-dihydro-9,10-diboraanthracene formed complexes with fluoride ions, resulting in the change of the absorption and fluorescence.

Acknowledgments

This work was partially supported by Grants-in-Aid for the Global COE Program (Chemistry Innovation through Cooperation of Science and Engineering) and for the Scientific Researches from MEXT and JSPS. We also thank Tosoh Finechem Corp. for the generous gifts of alkyllithiums.

Supplementary data

Syntheses and characterization data of **2** and **3**; optimized geometry and plots of molecular orbitals of **3'** and $[3\text{-F}]^-$. Crystallographic data for the structural analysis have been deposited with the Cambridge Crystallographic Data Center (CCDC-774409). Copy of this information can be obtained free of charge from The Direc-

tor, CCDC, 12 Union Road, Cambridge CB2 1EZ, UK (Fax: +44 1223 336033; e-mail: deposit@ccdc.cam.ac.uk or <http://ccdc.cam.ac.uk>). Supplementary data associated with this article can be found, in the online version, at doi:10.1016/j.tetlet.2010.07.068.

References and notes

- (a) Entwistle, C. D.; Marder, T. B. *Chem. Mater.* **2004**, *16*, 4574; (b) Yamaguchi, S.; Tamao, K. *Chem. Lett.* **2005**, *34*, 2.
- (a) Yamaguchi, S.; Akiyama, S.; Tamao, K. *J. Am. Chem. Soc.* **2001**, *123*, 11372; (b) Sundararaman, K.; Venkatasubbaiah, K.; Victor, M.; Zakharov, L. N.; Rheingold, A. L.; Jäkle, F. *J. Am. Chem. Soc.* **2006**, *128*, 16554; (c) Zhou, G.; Baumgarten, M.; Müllen, K. *J. Am. Chem. Soc.* **2008**, *130*, 12477; (d) Day, J. K.; Bresner, C.; Coombs, N. D.; Fallis, I. A.; Ooi, L.-L.; Aldridge, S. *Inorg. Chem.* **2008**, *47*, 793; (e) Agou, T.; Sekine, M.; Kobayashi, J.; Kawashima, T. *Chem. Commun.* **2009**, 1894; (f) Agou, T.; Sekine, M.; Kobayashi, J.; Kawashima, T. *J. Organomet. Chem.* **2009**, *694*, 3833.
- (a) Chen, J.; Kampf, J. W.; Ashe, A. J., III *Organometallics* **2008**, *27*, 3639; (b) Chai, J.; Wang, C.; Jia, L.; Pang, Y.; Graham, M.; Cheng, S. Z. D. *Synth. Met.* **2009**, *159*, 1443; (c) Akutsu, H.; Kozawa, K.; Uchida, T. *Synth. Met.* **1995**, *70*, 1109.
- (a) Metz, M. V.; Schwartz, D. J.; Stern, C. L.; Nickias, P. N.; Marks, T. J. *Angew. Chem., Int. Ed.* **2000**, *39*, 1312; (b) Metz, M. V.; Schwartz, D. J.; Stern, C. L.; Marks, T. J. *Organometallics* **2002**, *21*, 4159; (c) Williams, V. C.; Dai, C.; Li, Z.; Collins, S.; Piers, W. E.; Clegg, W.; Elsegood, M. R. J.; Marder, T. B. *Angew. Chem., Int. Ed.* **1999**, *38*, 3695.
- Lorbach, A.; Bolte, M.; Li, H.; Lerner, H.-W.; Holthausen, M. C.; Jäkle, F.; Wagner, M. *Angew. Chem., Int. Ed.* **2009**, *48*, 4584.
- Lorbach, A.; Bolte, M.; Lerner, H.-W.; Wagner, M. *Chem. Commun.* **2010**, 3592.
- (a) Müller, P.; Pritzkow, H.; Siebert, W. *J. Organomet. Chem.* **1996**, *524*, 41; (b) Müller, P.; Gangnus, B.; Pritzkow, H.; Schulz, H.; Stephan, M.; Siebert, W. *J. Organomet. Chem.* **1995**, *487*, 235.
- (a) Bieller, S.; Zhang, F.; Bolte, M.; Bats, J. W.; Lerner, H.-W.; Wagner, M. *Organometallics* **2004**, *23*, 2107; (b) Müller, P.; Huck, S.; Köppel, H.; Pritzkow, H.; Siebert, W. *Z. Naturforsch. B* **1995**, *50*, 1476; (c) Eisch, J. J.; Kotowicz, B. W. *Eur. J. Inorg. Chem.* **1998**, 761.
- Compound **3** was synthesized by a different method. See Ref. 7b.
- Sheldrick, G. M. *SHELX-97, Program for the Solution of Crystal Structure*; University of Göttingen, 1997.
- Zettler, F.; Hausen, H. D.; Hess, H. *J. Organomet. Chem.* **1974**, *72*, 157.
- DFT calculations at B3LYP level of theory were performed on model compounds **3'** and $[3\text{-F}]^-$ bearing 2,6-dimethylphenyl groups instead of mesityl groups in real molecules **3** and $[3\text{-F}]^-$ using GAUSSIAN 03 program package, and 6-31G(d) and 6-31G+(d) level of theory were employed for geometry optimization and single point calculations, respectively. Frisch, M. J.; Trucks, G. W.; Schlegel, H. B.; Scuseria, G. E.; Robb, M. A.; Cheeseman, J. R.; Montgomery, J. A., Jr.; Vreven, T.; Kudin, K. N.; Burant, J. C.; Millam, J. M.; Iyengar, S. S.; Tomasi, J.; Barone, V.; Mennucci, B.; Cossi, M.; Scalmani, G.; Rega, N.; Petersson, G. A.; Nakatsuji, H.; Hada, M.; Ehara, M.; Toyota, K.; Fukuda, R.; Hasegawa, J.; Ishida, M.; Nakajima, T.; Honda, Y.; Kitao, O.; Nakai, H.; Klene, M.; Li, X.; Knox, J. E.; Hratchian, H. P.; Cross, J. B.; Bakken, V.; Adamo, C.; Jaramillo, J.; Gomperts, R.; Stratmann, R. E.; Yazyev, O.; Austin, A. J.; Cammi, R.; Pomelli, C.; Ochterski, J. W.; Ayala, P. Y.; Morokuma, K.; Voth, G. A.; Salvador, P.; Dannenberg, J. J.; Zakrzewski, V. G.; Dapprich, S.; Daniels, A. D.; Strain, M. C.; Farkas, O.; Malick, D. K.; Rabuck, A. D.; Raghavachari, K.; Foresman, J. B.; Ortiz, J. V.; Cui, Q.; Baboul, A. G.; Clifford, S.; Cioslowski, J.; Stefanov, B. B.; Liu, G.; Liashenko, A.; Piskorz, P.; Komaromi, I.; Martin, R. L.; Fox, D. J.; Keith, T.; Al-Laham, M. A.; Peng, C. Y.; Nanayakkara, A.; Challacombe, M.; Gill, P. M. W.; Johnson, B.; Chen, W.; Wong, M. W.; Gonzalez, C.; Pople, J. A. *GAUSSIAN 03, Revision C.02*; Gaussian: Wallingford, CT, 2004.
- Wakamiya, A.; Mori, K.; Araki, T.; Yamaguchi, S. *J. Am. Chem. Soc.* **2009**, *131*, 10850.
- 9,10-Dihydro-9,10-diboraanthracene derivatives bearing smaller substituents on the boron atoms were reported to form complexes with THF, resulting in blue-shift of the absorption maxima unlike **3**. See Ref. 3b.
- HOMO, HOMO-1, HOMO-2, and HOMO-3 of **3** were mixtures of occupied π -orbitals of the mesityl groups, and the highest occupied π -orbital on the 9,10-dihydro-9,10-diboraanthracene skeleton was found as HOMO-4. On the other hand, LUMO and LUMO+1 of **3** were π orbitals of 9,10-dihydro-9,10-diboraanthracene formed by the mixing of 2p (B) orbitals and π orbitals of the benzene rings. See the Supplementary data for detail.
- Because the complexation constant was too large, the estimation quality was not good.
- The reaction of **3** and excess amount of $(n\text{-Bu})_4\text{NF}$ (6 equiv) in THF- d_6 seemed to afford only monofluoroborate $[3\text{-F}]^-$, judging from ^1H NMR spectrum, even at low temperature (193 K). However, negative-mode FAB-MS of this mixture showed ion peaks at m/z 693 and 451 that correspond to $(n\text{-Bu}_4\text{N})^+$ or H^+ adduct of difluoroborate $[3\text{-2F}]^{2-}$, respectively. The presence of the isosbestic point in the reaction of $[3\text{-F}]^-$ and more than 1 equiv of fluoride ion further indicates the formation of the difluoroborate. If the formation of the difluoroborate is supposed, its formation constant was calculated to be $K = 1.4(8) \times 10^6 \text{ M}^{-1}$.
- The fluorescence quantum yields after the complexation were estimated by a comparative method based on the absolute value for **3** in THF (0.05).